

# Method of Images for a Charge inside a Three-Layer Medium and Implementation of a Dirichlet Border Condition

Valencia, Fausto<sup>1\*</sup> ; Arcos, Hugo<sup>1</sup> 

<sup>1</sup>Escuela Politécnica Nacional, Faculty of Electrical Engineering, Quito, Ecuador

**Abstract:** A process to apply the method of images for a charge located in a three-layer medium is presented. The images are found according to the boundary conditions between the layers for the electric field. The characteristics of the electric potential are also considered, thus the number of unknown variables becomes a guide to set the image charges needed to solve the problem. The results are compared with finite element simulations through the use of the software FEMM 4.2, showing good agreement. The found limitations of the process are also noted, mainly in regards to the dependence of the images on the coordinates where the field is to be calculated. The model obtained was applied to different cases, where it was seen that it was not limited to three material media only. Finally, the null potential boundary condition was applied, showing how the method of images could be applied to this type of problems.

**Keywords:** Computational electromagnetics, electrostatic analysis, electric potential, nonhomogeneous media, numerical models, permittivity.

## Método de las Imágenes para una Carga en un Medio de Tres Capas e Implementación de la Condición de Dirichlet

**Resumen:** En el presente artículo, se presenta un proceso para aplicar el método de las imágenes en una carga localizada en un medio de tres capas de diferente permitividad. Las imágenes se determinan mediante el análisis de las condiciones de borde del campo eléctrico entre diferentes capas. También se considera el comportamiento del potencial eléctrico, de esta manera, se logra tener el mismo número de ecuaciones y de incógnitas para la determinación del valor de las imágenes. Los resultados del método propuesto se contrastan con los obtenidos mediante la aplicación del método de elementos finitos con el programa FEMM 4.2. Se presentan también las limitaciones del método, principalmente relacionadas con la dependencia del valor de carga de las imágenes con las coordenadas donde se calcula el potencial. El modelo obtenido fue aplicado a diferentes casos, donde se observó que el mismo puede ser utilizado para problemas de una y dos capas. Finalmente, se implementó la condición de Dirichlet, en la cual se aplicó un voltaje nulo a una de las fronteras, con lo cual se demostró que el método de las imágenes también puede ser utilizado en este tipo de problemas.

**Palabras clave:** Métodos computacionales en electromagnetismo, análisis electrostático, potencial eléctrico, medios no homogéneos, modelos numéricos, permitividad.

### 1. INTRODUCTION

Electrostatics is an important subject of Electromagnetic Theory that contributes to the understanding of complex phenomena and industrial applications such as high voltage breakdown (Abdel, 2018), aerosol particles (Kawada, 2002), or the analysis of molecular surfaces (Bulat, 2010). For this reason, some numerical techniques to solve electrostatics problems have been developed and are still under investigation. See, for example (Tausch, 2001) for the Method of Moments, (Karkkainen, 2001) for the Finite Difference Method or (Hamou, 2015) for the Finite Element Method. The Finite Element Method (FEM) is the most used method in electromagnetics research as it may be seen in the number of publications found in the scientific community. It solves the Laplace equation, taken as a boundary-value problem (Jin, 2017). However, this very characteristic of being able to solve bounded problems is, sometimes, its weakest feature, because

solving unbounded problems could become extremely difficult; in fact, some attempts are still being done to solve unbounded problems as seen in (Cao, 2016).

On the other hand, the Method of Images (MOI) is very suitable to solve unbounded problems, which is the reason why it has been used in the analysis of transmission lines (Bracken, 1976), or grounding systems (Dawalibi, 1994). But the method has not been developed for bounded problems, which is a great disadvantage in regards with the bounded methods seen before. This has made the method to be disregarded even though it has good features like speed of solution or implementation simplicity.

In the face of that, this paper shows a process to get the images for a charge located inside a medium that contains three different materials. Then, the model is simplified in order to apply a null potential boundary condition.

fausto.valencia@epn.edu.ec

Recibido: 18/07/2019

Aceptado: 10/12/2019

Publicado: 31/01/2020

10.33333/tp.vol44n2.01

## 2. DETERMINATION OF THE CHARGE IMAGES

A charge is immersed in a three-layer medium, with permittivity  $\epsilon_1, \epsilon_2$ , and  $\epsilon_3$ , as seen in Figure 1. The charge is located in the first layer, at the point  $(d, x)$ , the second layer is  $h$  meters width, and the third layer goes towards infinity. The purpose of this analysis is to obtain the electric field and the electric potential on each layer. The procedure is an extension of that presented in (Jackson, 1975).

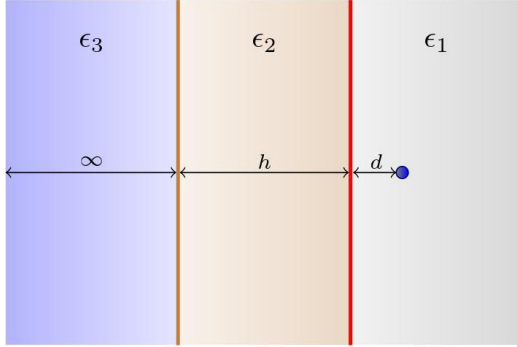


Figure 1. Charge in a three-layer medium

The equations governing the system under analysis, where there is a field  $E$  and a charge density  $\rho$ , are:

$$\begin{aligned} \nabla \times \mathbf{E} &= 0 && \text{The whole space} \\ \nabla \cdot \mathbf{E} &= \rho && \text{First layer} \\ \nabla \cdot \mathbf{E} &= 0 && \text{Second and third layers} \end{aligned} \quad (1)$$

The border conditions for the frontier between layer 1 (permittivity  $\epsilon_1$ ) and layer 2 (permittivity  $\epsilon_2$ ) are shown in (2) and (3), whereas those for the frontier between layers 2 and 3 (permittivity  $\epsilon_3$ ) are shown in (4) and (5).

$$\epsilon_1 E_{x1} = \epsilon_2 E_{x2} \quad (2)$$

$$E_{y1} = E_{y2} \quad (3)$$

$$\epsilon_2 E_{x2} = \epsilon_3 E_{x3} \quad (4)$$

$$E_{y2} = E_{y3} \quad (5)$$

From (1) to (5) the following criteria come out:

- The null rotational, that comes from the electrostatic nature of the problem, allows for the definition of a potential in all the regions considered.
- Due to the presence of charge only on the first layer, the original charge must be considered exclusively on that layer.
- There are four border conditions, two per each layer division. Hence, four charge images are needed to represent the whole problem.

The four charge images interact with the potential in the way shown in Table I, where  $\Phi_i$  is the potential for the layer  $i$ .

Accordingly, the four images are located as shown in Figure 2. The charge images should be symmetrical at most as possible

to reduce the effect of the  $y$  coordinate. As a consequence, the images  $q_2, q_4$  stay at the same point of the original charge  $q_0$ , although their values are not necessarily the same.

Table 1. Characteristics of the Charge Images

Charge Image	Symmetrical to	Potential of influence
$q_1$	$q_0$ around the border from layer 1 to layer 2	$\Phi_1$
$q_2$	$q_1$ around the border from layer 1 to layer 2	$\Phi_2$
$q_3$	$q_0$ around the border from layer 2 to layer 3	$\Phi_1, \Phi_2$
$q_4$	$q_3$ around the border from layer 2 to layer 3	$\Phi_3$

With all those considerations, the potential  $\Phi$  for each layer is:

$$\begin{aligned} \Phi_1 &= \frac{1}{4\pi\epsilon_1\epsilon_0} \left( \frac{q_0}{R_0} + \frac{q_1}{R_1} + \frac{q_3}{R_3} \right) \\ \Phi_2 &= \frac{1}{4\pi\epsilon_2\epsilon_0} \left( \frac{q_2}{R_2} + \frac{q_3}{R_3} \right) \\ \Phi_3 &= \frac{1}{4\pi\epsilon_3\epsilon_0} \frac{q_4}{R_4} \end{aligned} \quad (6)$$

The position vectors, according to Figure 2, are:

$$\mathbf{R}_0 = (x - d)\mathbf{e}_x + y\mathbf{e}_y$$

$$\mathbf{R}_1 = (x + d)\mathbf{e}_x + y\mathbf{e}_y$$

$$\mathbf{R}_2 = \mathbf{R}_4 = \mathbf{R}_0$$

$$\mathbf{R}_3 = (x + d + 2h)\mathbf{e}_x + y\mathbf{e}_y$$

The electric field  $\mathbf{E}$  is determined by:

$$\mathbf{E} = \nabla\Phi \quad (8)$$

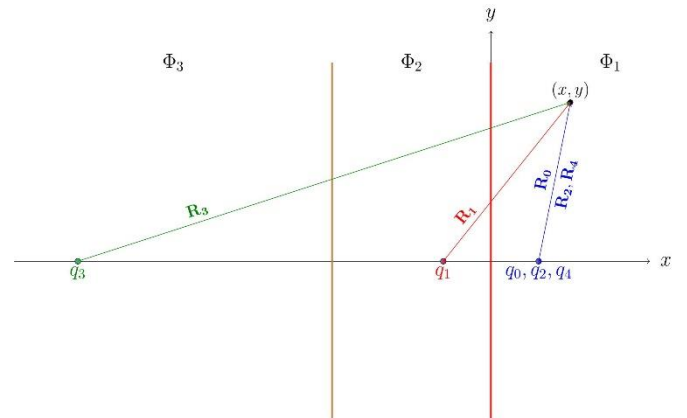


Figure 2. Location of the four charge images and the original charge. The position vectors for the electrostatic analysis in the point  $(x, y)$  are also included.

After applying (8), the electric fields for each layer are found with (9). In its derivation, we assumed that the charge images do not vary with any coordinate, neither  $x$  nor  $y$ . However, after solving the system, it was seen that they indeed depend on the coordinates. Even so, that dependence resulted to be negligible for the case under analysis, and the assumption made in the derivation could be taken for certain.

Nonetheless, each problem should be tested, mainly when the value of the charge inside the first layer is in the order of units of coulombs.

The border conditions are considered in (9). In  $x = 0$ , (2) and (3) were applied, noting that the module of the vector  $R_0 = R_1$ . On the other hand, in  $x = -h$  the conditions (4) and (5) prevail, with  $R_0 = R_3$  at this line. Then, the system of equations (10) is obtained.

After the system is solved, the charge images can be used in (6) and (9) to get the potential and the electric field.

$$\begin{aligned}
 E_{x1} &= \frac{1}{4\pi\epsilon_1\epsilon_0} \left[ \frac{q_0(x-d)}{R_0^3} + \frac{q_1(x+d)}{R_1^3} + \frac{q_3(x+d+2h)}{R_3^3} \right] \\
 E_{y1} &= \frac{1}{4\pi\epsilon_1\epsilon_0} \left[ \frac{q_0y}{R_0^3} + \frac{q_1y}{R_1^3} + \frac{q_3y}{R_3^3} \right] \\
 E_{x2} &= \frac{1}{4\pi\epsilon_2\epsilon_0} \left[ \frac{q_2(x-d)}{R_2^3} + \frac{q_3(x+d+2h)}{R_3^3} \right] \\
 E_{y2} &= \frac{1}{4\pi\epsilon_2\epsilon_0} \left[ \frac{q_2y}{R_2^3} + \frac{q_3y}{R_3^3} \right] \\
 E_{x3} &= \frac{1}{4\pi\epsilon_3\epsilon_0} \left[ \frac{q_4(x-d)}{R_4^3} \right] \\
 E_{y3} &= \frac{1}{4\pi\epsilon_3\epsilon_0} \left[ \frac{q_4y}{R_4^3} \right] \\
 q_1 + q_2 &= q_0 \\
 q_1 - \frac{\epsilon_1}{\epsilon_2} q_2 + \frac{\epsilon_2 - \epsilon_1}{\epsilon_2} \cdot \frac{R_0^3}{R_3^3} \Big|_{x=0} q_3 &= -q_0 \\
 -q_2 + q_3 + q_4 &= 0 \\
 q_2 + q_3 - \frac{\epsilon_2}{\epsilon_3} q_4 &= 0
 \end{aligned} \tag{9}$$

### 3. DIRICHLET NULL POTENTIAL CONDITION

If compared with the Finite Element Method, the Method of Images has the disadvantage of not being suitable to treat borders with fixed potential, which are known as Dirichlet border condition. On the other hand, the Method of Images has

the advantage of solving open boundary problems, which is somehow complicated for the Finite Element Method. In order to face this issue, in this research, we used the results of the three-layer model to get a Dirichlet null potential condition in a two-layer medium.

The null potential was placed at  $x = -h$ , i.e. on the division between the second and third layer. As a result, and to have the same behavior shown by Finite Element simulations, the whole third layer should have a potential of zero volts. In (6), this could be accomplished by setting  $q_4 = 0$  or  $\epsilon_3 \rightarrow \infty$ . The first option brings out some inconsistencies in the border equations (2) to (4). Hence, we opted for the use of the second option by giving an infinite value to the third permeability.

As a parallel consequence, the border conditions force the  $y$  component to disappear, since there is no field in the third layer. The same is not truth for the  $x$  component, because, as seen in (4), the ratio between the field components in both layers is given by the ratio between each permeability, and so, at infinite permeability,  $E_{x2}$  could exist, even though  $E_{x3}$  is zero.

## 4. RESULTS

### 4.1. Comparison with the finite element method

The results of the Method of Images are compared with those of the software FEMM 4.2 which uses the Finite Element Method.

#### a) Three - layer médium

A charge of  $1 \mu C$ , at a distance  $d = 0.1 m$  from the division between the first and the second layer is analysed. The second layer has a width  $h = 1 m$ . The first layer has a relative permittivity of 1, the second layer, 10, and the third layer, 50.

The implementation of the problem in FEMM 4.2 is shown in Figure 3. The problem has been set as axisymmetric, i.e. the geometry rotates around the vertical axis, thus building a sphere. The other option - rectangular geometry - could not be used because the method would create a line instead of a point charge.

Due to the characteristics of FEM, it was necessary to assume a null potential border, which in Figure 3 is represented by an external circle located at 30 m from the charge.

A detailed sample of the results for the potential is shown in Figure 4. The contour lines for the potential are shown at a radius of  $0.6 mm$ . It is not possible to show a larger area due to the high potential around the charge.

In this figure we could check the inaccuracies present due to the small features of the charge; note that the contours are far from being round locus. Besides, note that the contours are not perpendicular in the point of contact with the vertical axis; as a consequence, there is a horizontal component of the electric field in this point, which does not agree with the real case.

The results of simulations with FEM and MOI for the potential and the electric field are shown in Figure 5 and Figure 6 respectively. Note that those results are very similar, which suggest that the MOI model is close to the actual values. The maximum relative difference is 15% and for the potential and 34% for the electric field. Although those differences seem high, consider that FEM is not very suitable for the simulation of single charges.

#### b) Two-layer material with the Dirichlet condition

The same problem now is simulated setting the division of the second and third layer with a null potential, which is known as Dirichlet condition.

Figure 7 and Figure 8 show a good agreement between the results for FEM and MOI for the potential and the electric field respectively.

#### 4.2. Analysis of potential and electric field for different configurations

In this section, a charge inside different configurations of material is simulated. In order to show the versatility of the method, not all of the cases are for three-layer media.

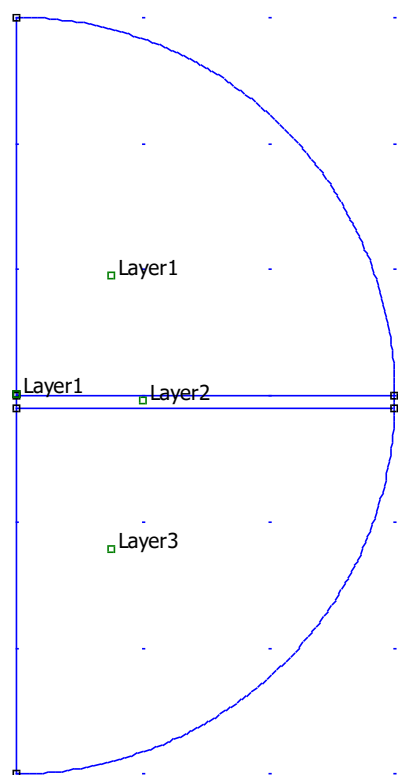


**Figure 3.** Implementation of the problem of one charge in a three-layer medium for the simulation in FEMM 4.2

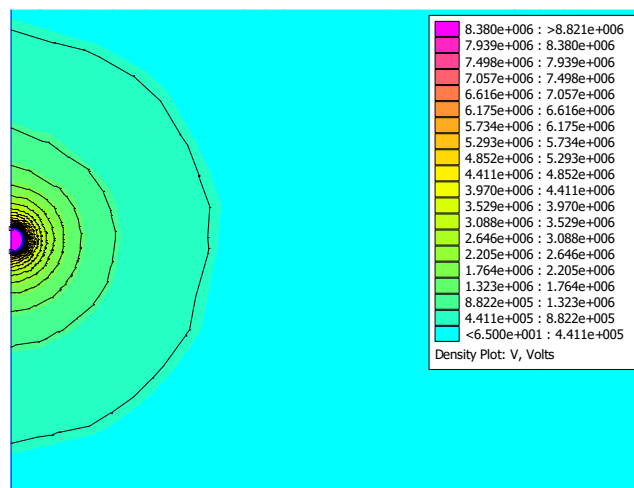


**Figure 4.** Equipotential lines and potential for the single charge in a three-layer medium.

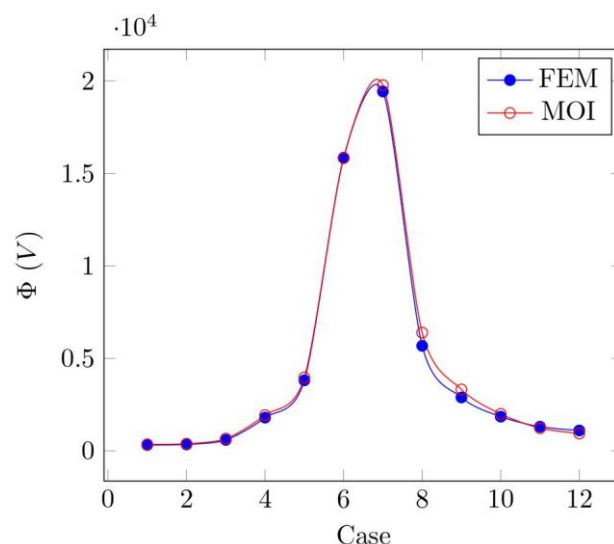


**Figure 5.** Results for simulation of a charge in a three-layer medium with the finite element method and the method of images.

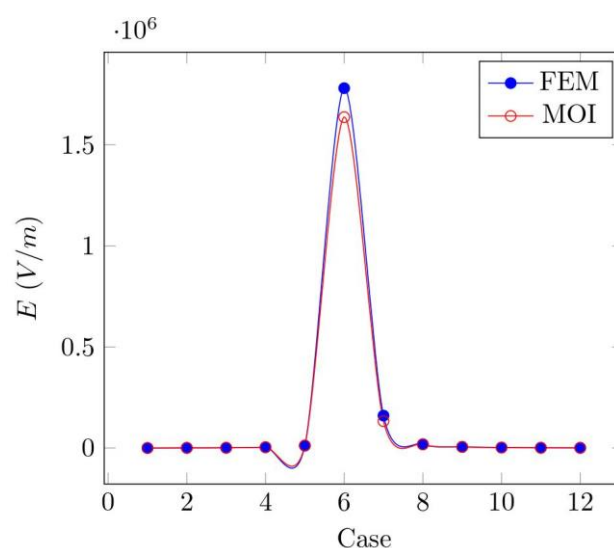


**Figure 6.** Results for the electric field of simulations with the finite element method and the method of images.

### a) Homogeneous medium

The homogeneous medium means that the permittivity is the same for the three-layers. The results are shown in Figure 9. As expected, the field lines go out from the charge and are perpendicular to the potential contours. There is no change in the field, due to the homogeneity of the medium.

### b) Two-layer medium $\epsilon_1 < \epsilon_2$

The charge is now inside a medium with two different materials. The relative permittivity of the first layer is 1 and that of the second layer is 10. For three-layer model, this means to set the third and second permittivity with the same value. In this case, the charge was located at 0.5 m from the division of layers for a better appreciation of the results. Figure 10 shows the field and the potential.

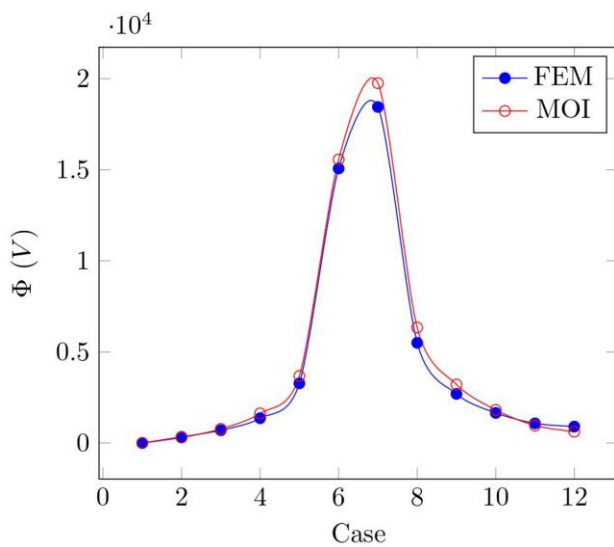


Figure 7. Results of the potential, simulated with FEM and MOI, when the second layer is grounded.

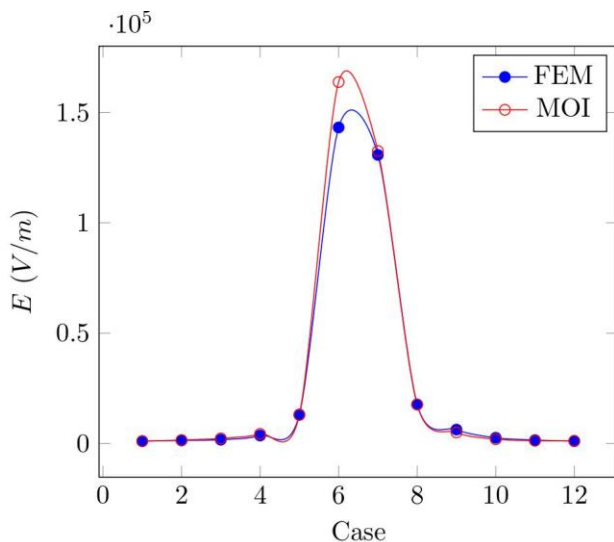


Figure 8. Results of the electric field, simulated with FEM and MOI, when the second layer is grounded

It is evident that the potential has a deviation when touching the second layer. In the same fashion, the electric field changes its direction and opens in the second layer. In the first layer,

the electric field, different from the homogeneous case, is somehow attracted to the second layer. The electric field is not perpendicular to the division of layers, which is logical since the second material is not a conductor.

### c) Two-layer medium: $\epsilon_2 < \epsilon_1$

The second layer has a relative permittivity of 1, and the first layer has one of 5. Figure 11 shows the results. The electric field is repelled from the division of layers, and is trying to be tangential at that division. Once the field enters the second layer, it reduces its slope and goes radially to the infinity.

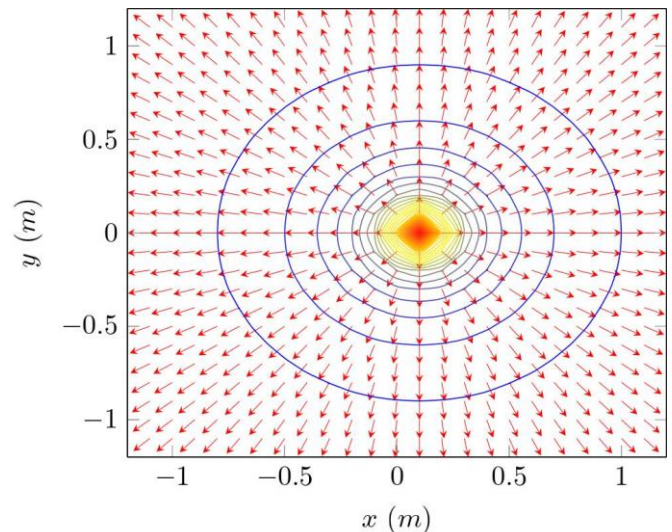


Figure 9. Electric field and potential for a charge on a homogeneous medium.

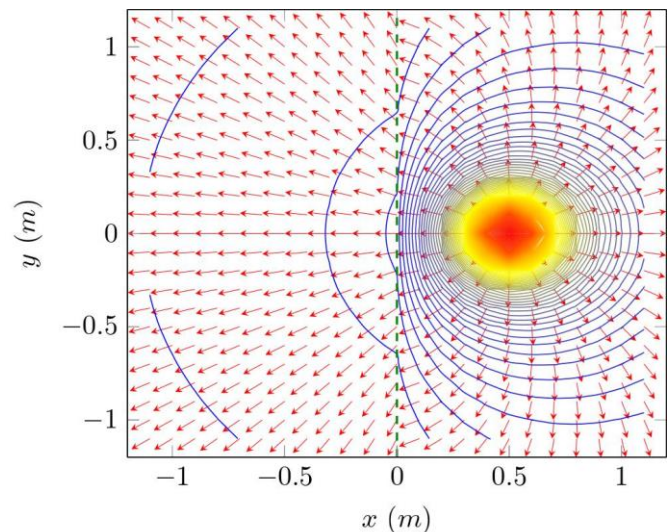


Figure 10. Electric field and potential for a charge inside a two-layer medium, where the permittivity of the first layer is less than that of the second layer.

### d) One layer with one extreme grounded

The relative permittivity of the first and second layers was set to 1, and that of the third layer was set to infinite.

The results are exposed in Figure 12. Note how the equipotential contours try to be parallel to the grounded line as



they are closer to it. Finally at the grounded line, the electric field becomes perpendicular.

*e) Three layers with different permittivity*

The most general case is simulated in this section. The medium contains three layers, each one of different permittivity: 1 for the first layer, 10 for the second layer and 5 for the third layer. Figure 13 shows the result.

In the potential contours we could see the sudden change when the field crosses each layer. In the first layer, the field is somehow attracted to the second layer.

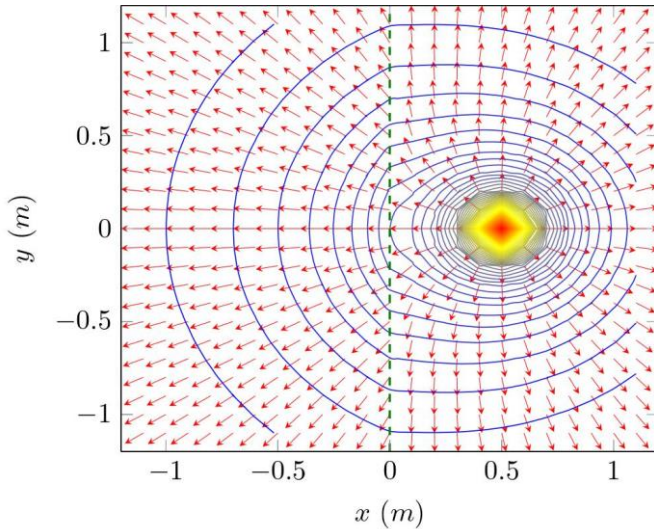


**Figure 11.** Electric field and potential for a charge inside a two-layer medium, where the permittivity of the first layer is greater than that of the second layer.

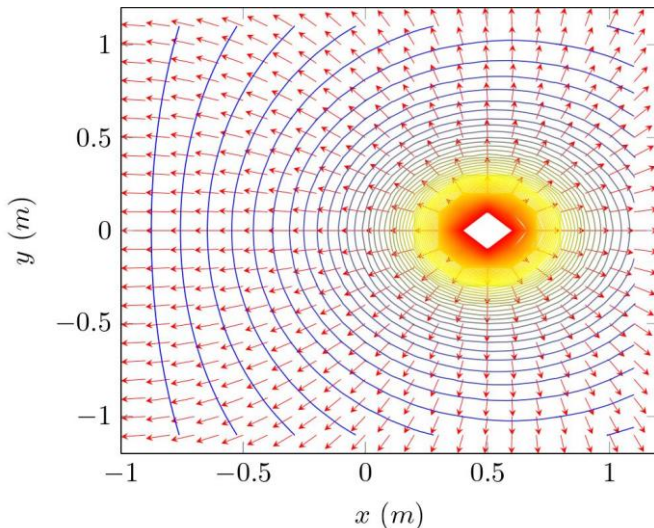


**Figure 12.** Electric field and potential contours for a charge in a homogeneous medium with the line ( $x=-1$ ) grounded.

*f) Two-layers with the second layer grounded*

The charge is immersed in a two-layer medium, the second layer is grounded in its farther side. The relative permittivity of the first layer is 1 and that of the second layer is 10, i.e. the two layers are the same as the case before.

The results are shown in Figure 14. The electric field is forced to be attracted towards the null potential, even though, as it was seen in the three-layer case, the field is usually going outside due to the higher permittivity of the second layer. A very important difference with the three-layer case is the influence of the null potential in the values of potential, which are seen to be closer to the charge.

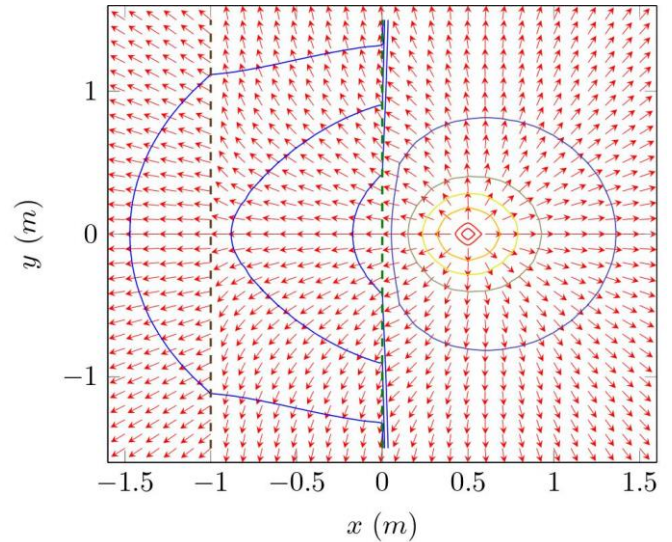


**Figure 13.** Electric field and potential contours for a charge inside a three-layer medium.

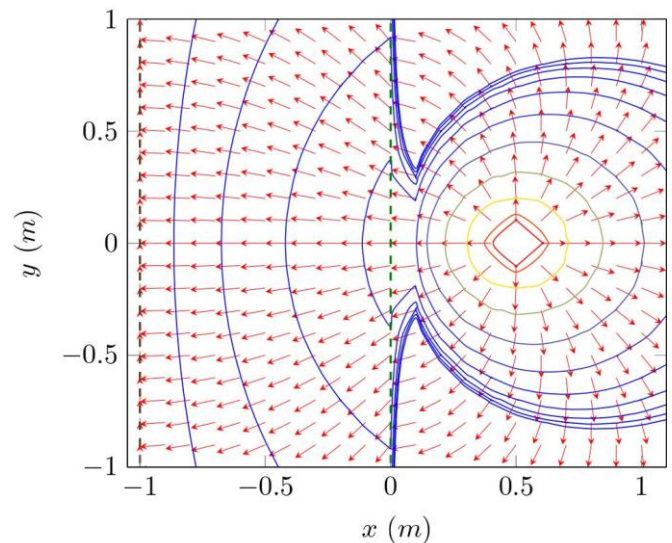


**Figure 14.** Electric field and potential contours for a charge inside a two-layer medium with the second layer grounded.

## 5. CONCLUSION

The method of images was successfully applied to a charge inside a three-layer medium. The model has good agreement with the finite element method, and in some extreme cases, represents better the real case, as it was seen when one of the components of the field does not exist.

Once the main equations for the field and potential are set, the determination of the images is straightforward. The implementation of the model does not require advance

programming techniques, because only basic operations are involved.

In the three-layer model, the images depend on the value of the  $y$  coordinate where the electrostatic values must be calculated. Although this characteristic could seem to be an obstacle for the application of the method, in the long term it did not affect the results, as it was seen when comparing with FEM.

The Dirichlet condition for a null potential was possible by setting the adequate value of permittivity in the related layer. Thus, by using this technique, the method of images could replicate some problems that are usually analysed only with boundary suited numerical methods. This is an important advantage that allows the method of images to solve bounded and unbounded problems, which is not so feasible in other numerical methods such as finite element or finite difference methods.

The process for the development of the method of images for a charge inside a three-layer medium could be extended to more layers and to different charge configurations, such as lines, capacitor plates, etc.

A complementary analysis could be the application of the process in the analysis of magnetostatic problems where the permeability is variable and the field is not radial but is solenoidal.

## REFERENCES

- Abdel-Salam, M. (2018). Electrical Breakdown in Gases, in *High-Voltage Engineering*. CRC Press.
- Bulat, F. A., Toro-Labbé, A., Brinck, T., Murray, J. S., & Politzer, P. (2010). Quantitative analysis of molecular surfaces: areas, volumes, electrostatic potentials and average local ionization energies. *Journal of molecular modeling*, 16(11), 1679-1691.
- Cao, Y., Chu, Y., Zhang, X., & Zhang, X. (2016). Immersed finite element methods for unbounded interface problems with periodic structures. *Journal of Computational and Applied Mathematics*, 307, 72-81.
- Dawalibi, F. P., Ma, J., & Southey, R. D. (1994). Behaviour of grounding systems in multilayer soils: a parametric analysis. *IEEE Transactions on Power Delivery*, 9(1), 334-342.
- Hamou, N., Massinissa, A., Hakim, A., & Youcef, Z. (2015). Finite element method investigation of electrostatic precipitator performance. *International Journal of Numerical Modelling: Electronic Networks, Devices and Fields*, 28(2), 138-154.
- Jackson, J. D., & Zia, R. K. (1977). Classical electrodynamics. *Physics Today*, 30, 61.
- Jin, J. M. (2015). Introduction to the Finite Element Method. *The finite element method in electromagnetics*. John Wiley & Sons.
- Karkkainen, K., Sihvola, A., & Nikoskinen, K. (2001). Analysis of a three-dimensional dielectric mixture with finite difference method. *IEEE Transactions on Geoscience and Remote Sensing*, 39(5), 1013-1018.
- Kawada, Y., Kaneko, T., Ito, T., & Chang, J. S. (2002). Simultaneous removal of aerosol particles, NO<sub>x</sub> and SO<sub>2</sub>, from incense smokes by a DC electrostatic precipitator with dielectric barrier discharge prechargers. *Journal of Physics D: Applied Physics*, 35(16), 1961.
- Tausch, J., Wang, J., & White, J. (2001). Improved integral formulations for fast 3-D method-of-moments solvers. *IEEE Transactions on Computer-Aided Design of Integrated Circuits and Systems*, 20(12), 1398-1405.

## BIOGRAFÍAS



**Fausto Valencia**, was graduated as Electrical Engineer and Master in Electrical Engineering both in the National Polytechnic School. He is a full time teacher and is currently developing the research towards obtaining the doctoral degree at the same institution. His fields of interest are high voltage, power system transients and the application of electromagnetic models in Electrical Engineering problems.



**Hugo Arcos Martínez**, born in Quito, Ecuador, in 1972. He received the Electrical Engineering degree at the National Polytechnic School in 1998, and PhD in Electrical Engineering at the National University of San Juan Argentina in 2003. He has developed his career professionals in various institutions of the Ecuadorian electricity sector and currently serves as Coordinator of the School of Electrical Engineering at the National Polytechnic School. His areas of interest are: Modeling in Electric Power Systems, Studies in steady state and transient and reliability SEP.

